IEEE Open Journal of
Industry Applications

Received 27 August 2021; revised 14 January 2022; accepted 30 January 2022. Date of publication 7 February 2022;
date of current version 24 February 2022. The review of this article was arranged by Associate Editor Petros Karamanakos.

Digital Object Identifier 10.1109/OJIA.2022.3148388

On Real-Time Hybrid Testing of Ocean Wave Energy Conversion Systems: An Experimental Study

ALI S. HAIDER [1] (Member, IEEE), TED K. A. BREKKEN [1], RYAN G. COE [2], GIORGIO BACELLI [2] (Member, IEEE), AND ALAN MCCALL [3]

[1] School of Electrical and Computer Engineering, Oregon State University, Corvallis, OR 97331 USA
[2] Water Power Technologies Department, Sandia National Laboratories, Albuquerque, NM 87185 USA
[3] Dehlsen Associates, LLC., Santa Barbra, CA 93101 USA

CORRESPONDING AUTHOR: ALI S. HAIDER (e-mail: haidera@oregonstate.edu).

ABSTRACT The growing wave energy sector requires an efficient and flexible testing process for the development phase of wave energy systems. Real-time hybrid testing is a promising technique for the accelerated testing of wave energy conversion systems. This article presents an experimental study on developing a hybrid testing platform for wave energy systems at the Wallace Energy System and Renewables Facility (WESRF) at Oregon State University. The wave energy conversion system is broken down into numeric (i.e., virtual) and physical (i.e., hardware) components. The numeric component involves software components such as the control algorithm for Wave Energy Converter (WEC) and controller for the power electronic converters and numerical models for the WEC device hydrodynamics. The hardware involves an ocean wave emulator testbed, Power Take-Off (PTO) mechanism, power electronics, and instrumentation. The numeric components are implemented in a real-time target machine and are interfaced with the experimental system. A case study implementation of Nonlinear Model Predictive Control (NMPC) is presented for a single degree of freedom heaving nonlinear WEC model with a Permanent Magnet Synchronous Generator (PMSG) as a PTO system. A Field-Oriented Control (FOC) algorithm controls the PMSG-PTO generation using a three-phase Integrated Intelligent Power (IIP) module converter. A demonstration of the proposed hybrid testing setup is provided.

INDEX TERMS Nonlinear model predictive control, field-oriented control, power converter, nonlinear power take-off, real-time hybrid testing, wave energy converter.

I. INTRODUCTION

Renewable energy technologies present a sustainable, low-carbon solution to growing global energy demands. The ocean provides a potential for an untapped energy resource for the world's increasing appetite for energy, with its low environmental effect and greater energy density [1], [2]. Ocean wave energy is converted to mechanical energy by Wave Energy Converter (WEC) devices. Among WEC devices, point absorbers (floating buoys) are promising solutions to capture wave energy [3], [4]. Conversion of mechanical energy to electrical energy requires Power Take-Off (PTO) mechanisms. The control strategy of PTO systems needs to ensure some energy conversion advantage within the system physical and operational constraints to ensure the economical operation of the wave energy conversion system. Therefore, optimal control of the PTO system is vital to the overall profitable operation of the WEC system. Among various control techniques for WEC are reactive control and latching [5], spectral methods, and pseudospectral techniques [6], [7]. Optimal control strategies have been explored in detail in the literature [2], [8].

Model Predictive Control (MPC) is an extensively studied controller strategy in this context [9]–[12]. MPC is an online

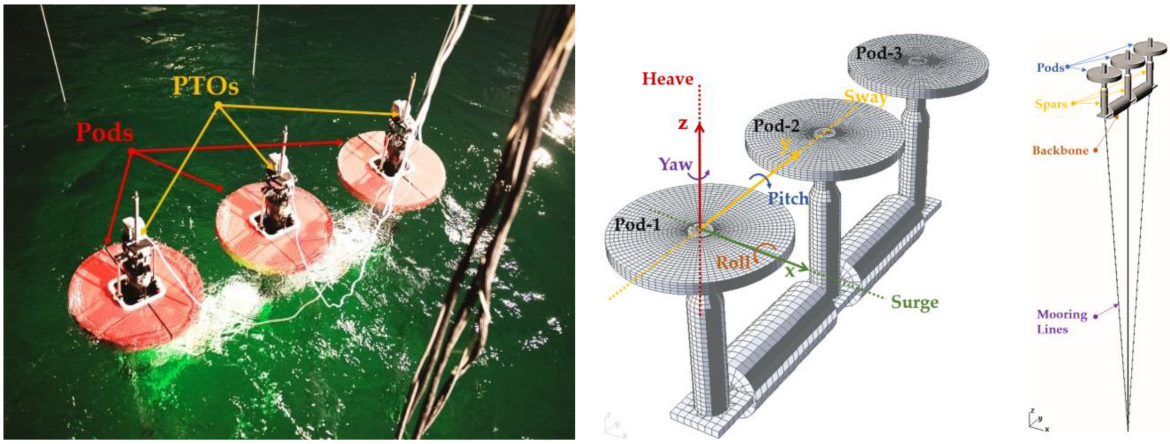

FIGURE 1. Image of the Dehlsen Associates, LLC, 1:35-scale CENTIPOD WEC: (a) WEC Model. (b) Baseline configuration. (c) Model with mooring lines.

optimization method that maximizes a cost index while respecting system constraints. Typically, the optimization objective of the MPC problem for WEC is to maximize the power capture by the PTO mechanism. However, other alternative formulations, such as Economic MPC [13], [14] are also explored to maximize economic operation metrics. Since MPC is a model-based control scheme, the system dynamics may be linear or include nonlinear effects, such as fluid viscous drag or mooring forces. Nonlinear MPC (NMPC) formulations have gained popularity because the WEC devices operate in non-ideal environments where nonlinear effects cannot be neglected. NMPC has also been investigated for WECs in literature. For example, an NMPC formulation based on differential flatness is presented in [15]. The nonlinear effects of mooring lines are presented in [9], and the effects of nonlinear fluid viscous drag are investigated in [16].

Moreover, the PTO mechanism is typically considered ideal. However, their reduced efficiency does negatively affect the optimal operation of the WEC system [17]–[19]. Some recent studies also consider the nonlinear PTO machine characteristics [20].

A more efficient and flexible testing process is needed to develop wave energy converter systems and the PTO mechanism for the growing wave energy sector [21]. Real-time hybrid testing is a promising technique for accelerated testing of WEC and PTO systems at their development phase. It involves breaking down the system into numerical and physical components and running the integrated hardware-software set up in real-time to access and evaluate the overall system performance [22]. Such accelerated testing techniques save product development costs, have been very successful in the automotive industry [23], and share some structural ideas with hardware-in-the-loop testing. These techniques are also gaining popularity in the WEC development sector [24], and hardware-in-the-loop (HIL) experiments can be a very powerful tool; for example, controller hardware-in-the-loop (CHIL) and power hardware-in-the-loop (PHIL) experimental testing for a renewable energy system integration [25]. The majority of the literature related to HIL focuses on experimental setups consisting of small scale rotatory motor-generator testbeds to simulate ocean hydrodynamics and wave energy converter dynamics [26]–[30], or hardware test rigs tailored for some particular type of WEC device, such as hydraulic PTO [31] and raft-type WEC [32], inertial mechanism-based WEC [33] and dielectric elastomer generators [34]. A limited amount of work is directed towards HIL testing of Linear PTO mechanisms, such as in [35], [36]; however, the scope of the work is limited to specific WEC in their facilities.

The degree of novelty of this work is related to the development of a more general-purpose hybrid testing platform at Wallace Energy Systems and Renewables Facility (WESRF) at the Oregon State University [37] for large scale WEC systems, with the capability to actuate a variety of Linear PTOs [38], [39] and rotary type PTO. Under Pacific Marine Energy Center (PMEC) [40], the test rig is available to academia, private industry, and national laboratories for collaborative research. Moreover, our work considers a nonlinear PTO efficiency model in NMPC implementation compared to ideal PTO models in most of the literature above.

This experimental study involves breaking down a case-study point absorber type WEC testing into numerical (i.e., virtual) models and physical (i.e., hardware) systems and running them in real-time to evaluate control techniques under numerous sea states. The hardware parts involve a scaled nonlinear PTO system coupled with a Linear Testbed (LTB) wave simulator, power electronics converters, electrical load, and sensors and instrumentation. The numeric component consists of a nonlinear model of a heaving WEC, the NMPC algorithm, and power electronics control. The numeric parts are implemented in real-time, which are interfaced with the various hardware components. The hybrid testing experiments

TABLE 1. Symbols for WEC Modeling

Symbol	Description
v_i	Velocity (Linear or Angular) in i^{th} DoF
x_i	Displacement (Linear or Angular) in i^{th} DoF
ξ_i	Intermediate State variables for radiation force State-Space approximation
$F_{r,pq}$	Radiation force in p^{th} DoF due to velocity in q^{th} DoF
$F_{hs,i}$	Hydrostatic force in i^{th} DoF
$F_{v,i}$	Viscous drag force in i^{th}DoF
$F_{e,i}$	Wave excitation force in i^{th}DoF
$F_{p,i}$	PTO force in i^{th}DoF
m	Mass of the float
$A_{pq}(\infty)$	Added mass at the infinite frequency in p^{th} DoF due to acceleration in q^{th} DoF
C_i	The hydrostatic restoring coefficient in i^{th} DoF
$C_{vd,i}$	Viscous drag coefficient in i^{th} DoF
A_{qp}	Frequency-dependent added mass in p^{th} DoF due to acceleration in q^{th} DoF
B_{qp}	Frequency-dependent damping in p^{th} DoF due to velocity in q^{th} DoF
K_{pq}	Radiation force impulse response without infinite frequency added mass
Z_{qp}	WEC Intrinsic impedance response in p^{th} DoF due to velocity in q^{th} DoF
a_i	Polynomial coefficients
$c_{i,j}$	Polynomial coefficients for cost functional
$I_{p,i}$	i^{th} PTO current
η_{Conv}	PTO converter efficiency
K_{Cu}	PTO generator copper loss constant
R_s	PTO generator winding resistance

are performed, and results of the successful performance of the hybrid platform are presented.

II. TIME DOMAIN MODEL OF A WAVE ENERGY CONVERTER

The Wave Energy Converter (WEC) device in this work is a full-scale version of the Dehlsen Associates, LLC multi-pod CENTIPOD [41], [42]. A 1:35-scale version of the device is shown in Fig. 1. This WEC device has three floating pods and three spars fixed to a single backbone structure. The backbone is anchored using mooring lines. This work selected a single pod from Fig. 1 for hybrid testing. We will follow the subscript notation of WEC-Sim Toolbox [43] for the degrees of freedom for WEC, in which the integers from 1, 2, …, 6 correspond to surge, sway, heave, roll, pitch, and yaw, respectively. Other notations and symbols for WEC modeling are given in Table I.

A. HEAVE DYNAMICS OF WEC

The Cummins equation for the heave dynamics of a point absorber pod is given by,

$$(m + A_{33}(\infty))\,\dot{v}_3(t) = -F_{r,33}(t) - F_{hs,3}(t) - F_{v,3}(t) - F_{p,3}(t) + F_{e,3}(t) \quad (1)$$

The hydrostatic, viscous damping, and radiation force terms in (1) are given by,

$$F_{r,33}(t) = \int_{-\infty}^{t} K_{33}(t-\tau)\, v_3 d\tau \quad (2)$$

$$F_{hs,3}(t) = C_3 x_3 \quad (3)$$

$$F_{v,3}(t) = C_{d,3} v_3 |v_3| \quad (4)$$

A transfer function expression can approximate the convolution integral term in (2),

$$F_{r,33}(t) = \int_{-\infty}^{t} K_{33}(t-\tau)\, v_3 d\tau = Z_{33}(j\omega) V_3(j\omega) \quad (5)$$

Using the device data from WAMIT [44], we can approximate the intrinsic impedance $Z_{pq}(j\omega)$ in (5) by a second-order transfer function using System Identification techniques,

$$Z_{33}(j\omega) = \left[j\omega\left(A_{33}(j\omega) - A_{33}(\infty)\right) + B_{33}(j\omega)\right] \approx \frac{\alpha_{33,1}s + \alpha_{33,0}}{s^2 + \beta_{33,1}s + \beta_{33,0}}\Big|_{s=j\omega} \quad (6)$$

The transfer function expression in (6) can be converted to a State-Space expression in Observer-Canonical form for the radiation force,

$$\begin{bmatrix}\dot{\xi}_1(t)\\ \dot{\xi}_2(t)\end{bmatrix} = \begin{bmatrix}0 & 1\\ a_1 & a_2\end{bmatrix}\begin{bmatrix}\xi_1(t)\\ \xi_2(t)\end{bmatrix} + \begin{bmatrix}b_1\\ b_2\end{bmatrix} v_3(t) \quad (7)$$

$$y_{33}(t) = \begin{bmatrix}1\ 0\end{bmatrix}\begin{bmatrix}\xi_1(t)\\ \xi_2(t)\end{bmatrix} = \xi_1(t) \approx F_{r,33}(t) \quad (8)$$

Defining a state vector for the WEC as

$$\mathbf{X} = \begin{bmatrix} v_3\ z_3\ F_{r,33}\ \xi_2 \end{bmatrix}^T \quad (9)$$

with $M_{33} = (m + A_{33}(\infty))$, and using (3), (4), (7), and (8) in (1), we get the following nonlinear state-space model for the WEC,

$$\dot{\mathbf{X}} = \mathbf{g}(\mathbf{X}, \mathbf{U}) = \begin{bmatrix} \frac{-C_3}{M_{33}}x_2 - \frac{1}{M_{33}}F_{r,33} - \frac{C_{d,3}}{M_{33}}v_3|v_3| - \frac{1}{M_{33}}F_{p,3} + \frac{1}{M_{33}}F_{e,3} \\ v_3 \\ b_1 v_3 + \xi_2 \\ b_1 v_3 + a_1 F_{r,33} + a_2 \xi_2 \end{bmatrix} \quad (10)$$

B. NONQUADRATIC WEC-PTO MODEL

For a given PTO generator, the electrical PTO power cost functional to be maximized, including the electrical losses, is given by,

$$\max_{F_{p,3}} P_{E,3} = \eta_{Conv}\left(P_{Mechanical,3} - P_{Loss,3}\right)$$

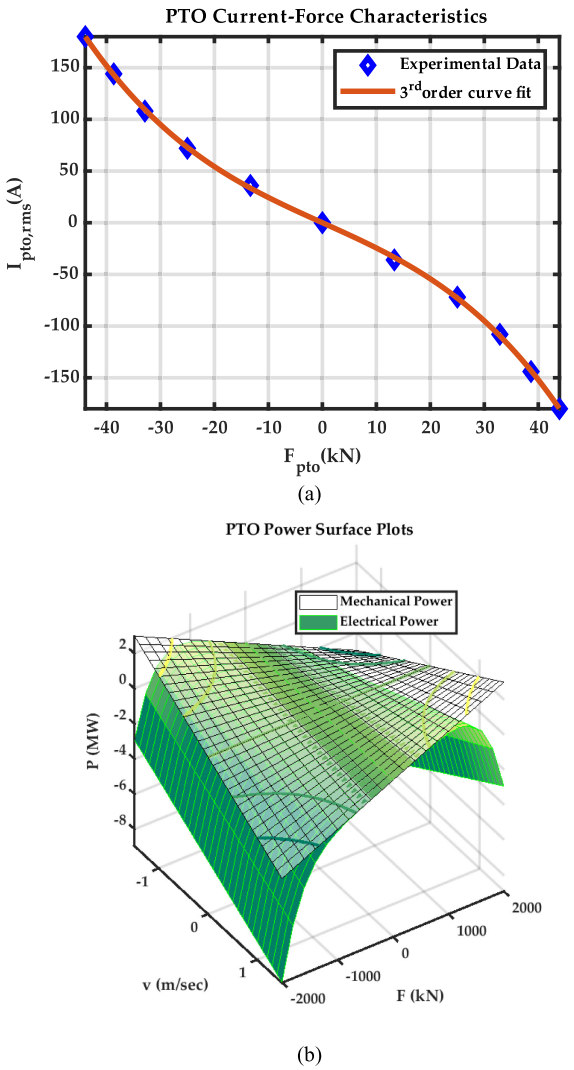

FIGURE 2. PTO generator force-current characteristics: (a) Polynomial curve fitting to the PTO force-current experimental data for a PTO generator. (b) Mechanical and electrical PTO power surface plot in PTO velocity-force plane.

$$= \eta_{Conv}\left(F_{p,3}v_3 - K_{Cu}\left[I_{p,3}\left(F_{p,3}\right)\right]^2 R_\Omega\right) \tag{11}$$

The case study scenario is taken from McCleer Power's Linear PTO generator [20] with the PTO generator force-current characteristics given by Fig. 2(a). We can approximate the experimental data in Fig. 2 is by a smooth third-order polynomial curve fit between the PTO current and the PTO force

$$I_{p,3}\left(F_{p,3}\right) = a_{33}F_{p,3}^3 + a_{23}F_{p,3}^2 + a_{13}F_{p,3} + a_{03} \tag{12}$$

Substituting (12) in (11), we get,

$$\begin{aligned} P_{E,3} = {} & c_{03}F_{p,3}v_3 \\ & - (c_{13}F_{p,3}^6 + c_{23}F_{p,3}^5 + c_{33}F_{p,3}^4 + c_{43}F_{p,3}^3 \\ & + c_{53}F_{p,3}^2 + c_{63}F_{p,3} + c_{73}) \end{aligned} \tag{13}$$

TABLE 2. Variable Description for NMPC Formulation

Symbol	Description
N	Prediction horizon
$\mathbf{X}$	State vector
$\rho_{N,i}$	Finite horizon terminal cost penalty or Mayer terms
$P_i(\cdot)$	Nonlinear functions or Lagrange terms
$\mathbf{p}$	A column vector of time-varying parameters
$\mathbf{U}$	PTO Force manipulated variable vector, $F_p(N)$
$\mathbf{d}$	Excitation force disturbance vector, F_e (N)
$q_k(t)$	Cost functional scheduling variable
R_i	Real numbers, such that $R_{k+1} > R_k$

The mechanical and electrical PTO surface plots from (11) are shown in Fig. 2(b). The mechanical power surface is non-convex, while the electrical power surface is convex due to the quadratic convexifying power loss term in (11).

III. IMPLEMENTATION OF NMPC FOR WEC

MPC is a model-based online optimal control solution, and a given NMPC problem optimizes a manipulated variable $\mathrm{u}(t)$ to maximize some cost functional $\mathrm{P}(\cdot)$ while respecting the system's physical constraints. A special class of NMPC problem has been formulated in [16], [20], in which the cost functional takes on a nonlinear piecewise polynomial form. Considering the case of finite-horizon optimization control, we can mathematically describe the NMPC problem of such a class as

$$\underset{\mathbf{u}(t)}{maximize}\ \mathbf{P}\left[t, \dot{\mathbf{X}}(t), \mathbf{X}(t), \mathbf{U}(t), \mathbf{p}(t)\right] \tag{14}$$

where

$$\mathbf{P}(\cdot) = \begin{cases} P_1(\cdot) + \rho_{N,1}(\cdot), & q_k(t) < R_1 \\ P_2(\cdot) + \rho_{N,2}(\cdot), & R_1 \le q_k(t) \le R_2 \\ \vdots & \vdots \\ P_j(\cdot) + \rho_{N,j}(\cdot), & R_{j-1} \le q_k(t) \le R_j \end{cases} \tag{15}$$

subjected to dynamic constraints,

$$0 = \mathbf{f}\left(t, \dot{\mathbf{X}}(t), \mathbf{X}(t), \mathbf{U}(t), \mathbf{d}(t), \mathbf{p}(t), N\right) \tag{16}$$

boundary constraint,

$$0 = \mathbf{r}\left(N, \mathbf{X}(0), \mathbf{U}(0), \mathbf{X}(N), \mathbf{U}(N), \mathbf{p}\right) \tag{17}$$

And path constraints,

$$0 \ge \mathbf{s}\left(t, \mathbf{X}(t), \mathbf{U}(t), \mathbf{p}(t)\right) \tag{18}$$

The description of various variables and constants in the control formulation (14) through (18) is given in Table II. The wave excitation force is an unmeasured disturbance and is estimated internally by the controller. For the NMPC problem for WEC, cost objective (14) takes the form of (11).

TABLE 3. PMSG PTO Generator Parameters

Symbol	Description	Value
P_r	Rated power	6000 W
V_r	Rated voltage	330 V
I_r	Rated current	15.7 A
ω_r	Rated speed	220 RPM
τ_r	Rated torque	347 $N.m$
P	Pole pairs	12
Ψ_{PM}	Permanent magnet flux linkage	1.194 Wb
τ_c	Cogging torque	3 $N.m$
J	Rotor inertia	0.245 $Kg.m^2$
R_s	Stator resistance	1.42 Ω
L_d, L_q	d and q axis inductance	30.50 mH

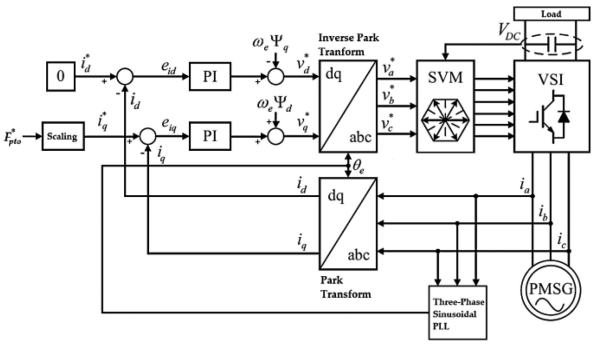

FIGURE 3. Schematic Diagram of Field-Oriented Control (FOC) for the PMSG-PTO generator.

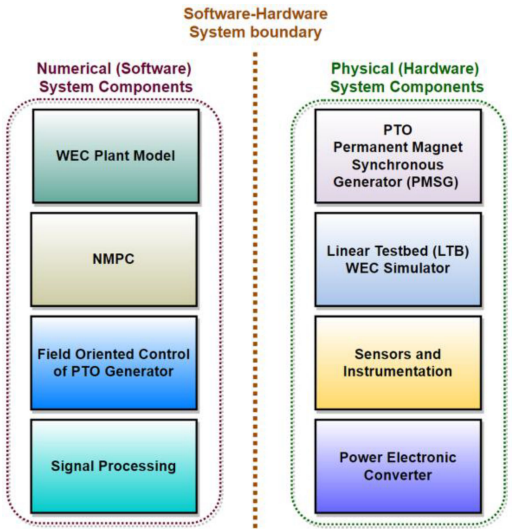

FIGURE 4. Hardware-Software system breakdown for the hybrid testing platform.

A. PREDICTION MODEL FOR NMPC

The NMPC algorithm optimizes a cost functional given by (11) that involves PTO current, a function of PTO force. We have developed an augmented model for WEC as a prediction model for the NMPC optimization problem. Defining the augmented state vector as

$$\mathbf{X_a} = \left[\, v_3 \;\; z_3 \;\; \xi_1 \;\; \xi_2 \;\; F_{p,3} \;\; I_{p,3} \,\right]^T \tag{19}$$

Using (10) and (12) along with the state definition (19), we get the following augmented model for the WEC for NMPC prediction, with $u_a = \dot{F}_{p,3}$ as the manipulated variable,

$$\begin{bmatrix} \dot{\mathbf{X}}_\mathbf{a} = \mathbf{g}\left(\mathbf{X_a}, u_a\right) = \frac{-C_3}{M_{33}} z_3 - \frac{1}{M_{33}} \\ F_{r,33} - \frac{C_{d,3}}{M_{33}} v_3 \left|v_3\right| - \frac{1}{M_{33}} F_{p,3} + \frac{1}{M_{33}} F_{e,3} \\ v_3 \\ b_1 v_3 + \xi_2 \\ b_1 v_3 + a_1 \xi_1 + a_2 \xi_2 \\ \dot{F}_{p,3} \\ 3a_{3,3} F_{p,3}^2 \dot{F}_{p,3} + 2a_{2,3} F_{p,3} \dot{F}_{p,3} + a_{1,3} \dot{F}_{p,3} \end{bmatrix} \tag{20}$$

The NMPC solves the nonlinear problem using MATLAB's built-in 'fmincon' function with the Sequential Quadratic Programming (SQP) algorithm [45], which outperforms every other tested method in terms of efficiency, accuracy, and percentage of successful solutions over a large number of test problems [46]. This function supports code generation for deployment on real-time target machines.

B. PMSG CONTROL STRATEGY

A Permanent Magnetic Synchronous Generator (PMSG) is used as a PTO generator. The PMSG is modeled in the dq-frame. The voltage equations for the generator in the dq-frame are given by,

$$v_d = R_s i_d + L_d \frac{di_d}{dt} - \omega_e L_q i_q \tag{21}$$

$$v_q = R_s i_q + L_q \frac{di_q}{dt} + \omega_e \Psi_{PM} + \omega_e L_d i_d \tag{22}$$

where ω_e is the electrical velocity, Ψ_{PM} is the permanent magnet flux linkage, and the subscripts d and q represent the direct and quadrature axis, respectively. The values of various parameters for the PMSG in (21) and (22) are summarized in Table III. The electromagnetic torque developed by the generator is given by,

$$\tau_{em} = \frac{3}{2} P \left(\Psi_{PM} i_q - \left(L_d - L_q\right) i_d i_q\right) \tag{23}$$

Since we use a surface-mounted PMSG, the d-axis and q-axis inductances are equal, and the dq-axis cross-coupling term in (23) vanishes. With a physical scaling parameter K_s, the PTO force relation can be obtained from (23) as,

$$F_{pto,PMSG} = K_s \tau_{em} = \frac{3}{2} K_s P \Psi_{PM} i_q \tag{24}$$

The d-axis current of the PTO PMSG is controlled using standard Field Oriented Control (FOC) [47]. The stator phase currents are converted to dq-axis currents using the Park transformation. The electrical angle θ_e and the electrical angular velocity ω_e are measured using a three-phase sinusoidal Phase

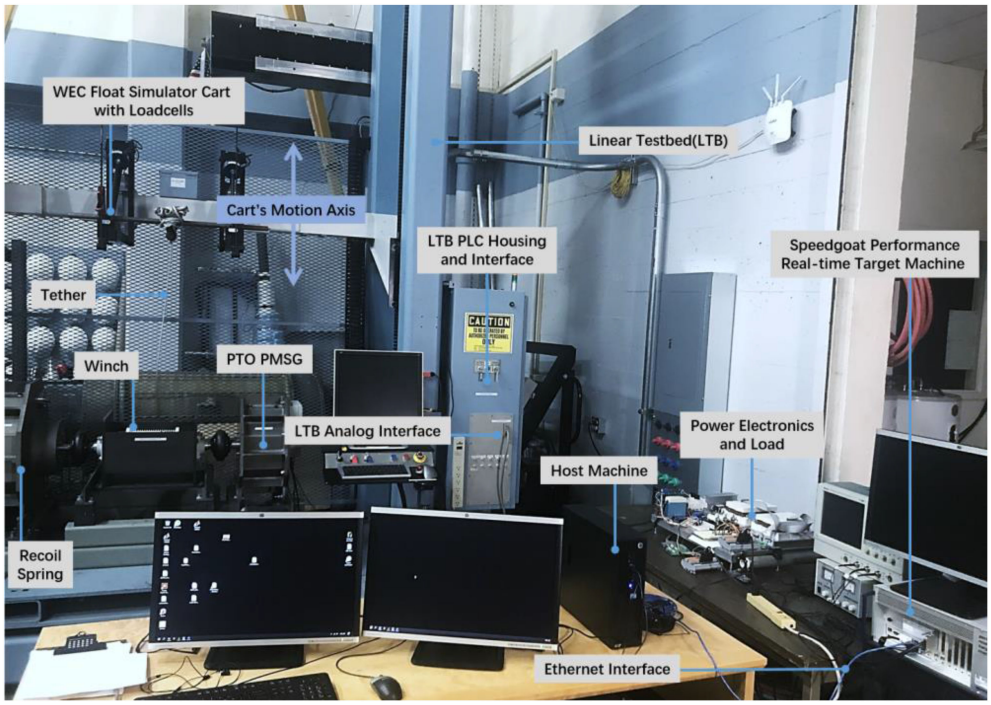

FIGURE 5. Experimental Setup for the hybrid testing platform.

Looked Loop (PLL). The commanded value of the d-axis current is zero, and the reference value of the q-axis current is calculated from (24). The PI controllers are used to convert current errors into dq-axis reference voltages. The DC link voltage is measured, and the dq-axis reference voltages are converted to PWM for the three-phase Voltage Source Inverter (VSI) using the Space Vector Modulation (SVM) technique. The schematic diagram for the FOC control method is shown in Fig. 3.

IV. HYBRID TESTING SCHEME

The hybrid testing involves breaking down the system into physical (i.e., hardware) and numeric (i.e., software) parts, as shown in Fig. 4.

The hybrid testing experimental setup is shown in Fig. 5. The control algorithm for the WEC, i.e., NMPC, and WEC plant dynamics, are implemented in the Speedgoat Performance real-time target machine [32], model-109100 with Intel Core i3 3.3 GHz, two cores, and 2048MB DDR3 RAM. The heave displacement of the WEC is commanded to the Linear Testbed (LTB) wave simulator machine [48] at the Wallace Energy Systems and Renewables Facility (WESRF) at Oregon State University. The heaving cart of LTB is tethered to the winch of a PTO generation mechanism, which is a PMSG coupled to a torsional restoring spring. NMPC acts as a high-level supervisory controller, solving its online optimization problem and issuing an optimal PTO force command at its sample time of 0.1 sec. The PTO force command is translated into q-axis current reference using (24). The PMSG-PTO generator is controlled using the q-axis current of its stator, using the low-level Field Oriented Control programmed in the Speedgoat machine with a sample time of 0.001 sec. We have used Semikron's SKiiP-603-GD123-3DUL-V3 three-phase IGBT Integrated Intelligent Power (IIP) modular bridge rectifier [49] as a Voltage Source Inverter (VSI) in Fig. 3. The actual PTO force output of PMSG is fed back to the NMPC. The WEC plant in Speedgoat receives the input PTO force from the loadcells on the LTB cart that monitor the tether tension in real-time. The schematic diagram of the hybrid testing scheme is shown in Fig. 6.

The Simulink model for code generation and deployment in the Speedgoat target machine for hybrid testing is shown in Fig. 7. The WEC model receives a preprogrammed real-time excitation force profile along with the PTO force signal from LTB's loadcells. The output displacement of WEC is commanded to LTB's Programmable Logic Controller (PLC) through Speedgoat's analogue channel, and WEC's displacement gets translated into the vertical displacement of LTB's cart. NMPC, as the higher-level controller, receives the augmented state vector and the physical measurement of the PMSG's PTO force and computes the next PTO force command. The PTO force control block in Fig. 7 scales the PTO force command to q-axis current reference and implements the Field-Oriented Control (FOC) as the low-level control to track the q-axis current command and generate the PWM signals through Speedgoat's PWM channels to drive the power converter.

The data acquisition and signal processing block in Fig. 7 reads various sensors and instruments and performs filtering and signal conditioning. It also implements a Phase-locked-Loop (PLL) on the three-phase current measurements and performs the Park transformation to compute the dq0-currents.

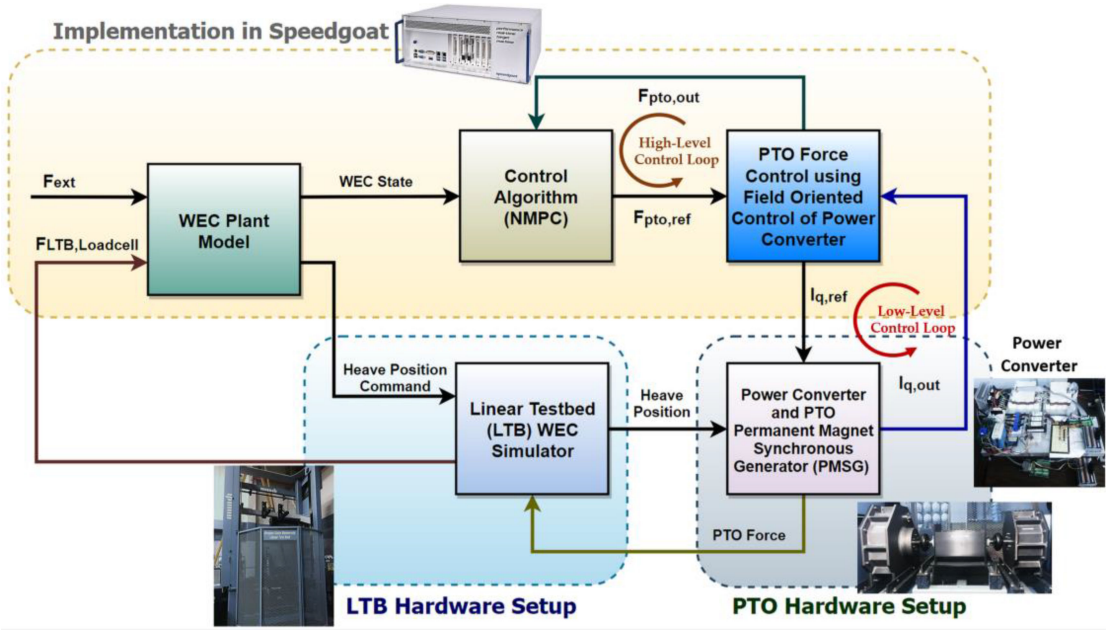

FIGURE 6. **Block diagram for the hybrid testing scheme.**

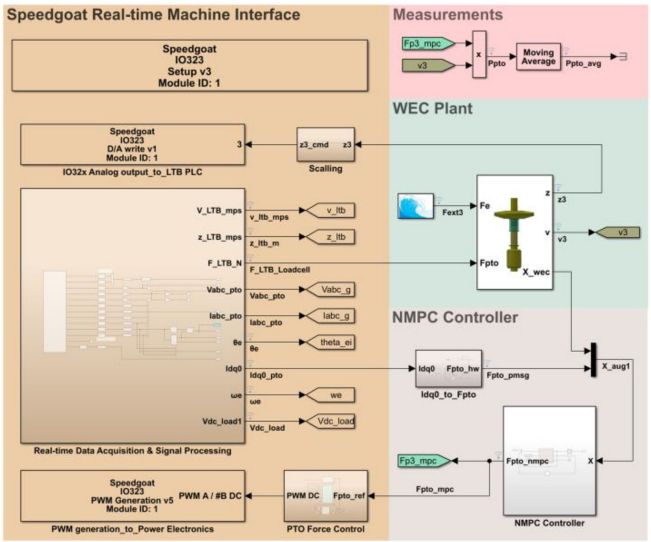

FIGURE 7. **Simulink model for the code generation and deployment in the Speedgoat target machine for hybrid testing.**

V. EXPERIMENTAL RESULTS AND DISCUSSION

The excitation force profile for the hybrid testing is shown in Fig. 8(a), which corresponds to an example sea state specified in Table IV.

A step time of 0.1 sec is used for NMPC formulation, close to one-tenth of the peak wave period, while a faster sampling time of 0.001 sec is selected for the PTO current control loop. The corresponding experimental WEC PTO-velocity and displacement are plotted in Fig. 8(b). The three-phase voltage and current outputs of the PMSG-PTO are shown in Fig. 9.

The PTO force commanded by NMPC and the corresponding output PTO force of PMSG is shown on the same plot

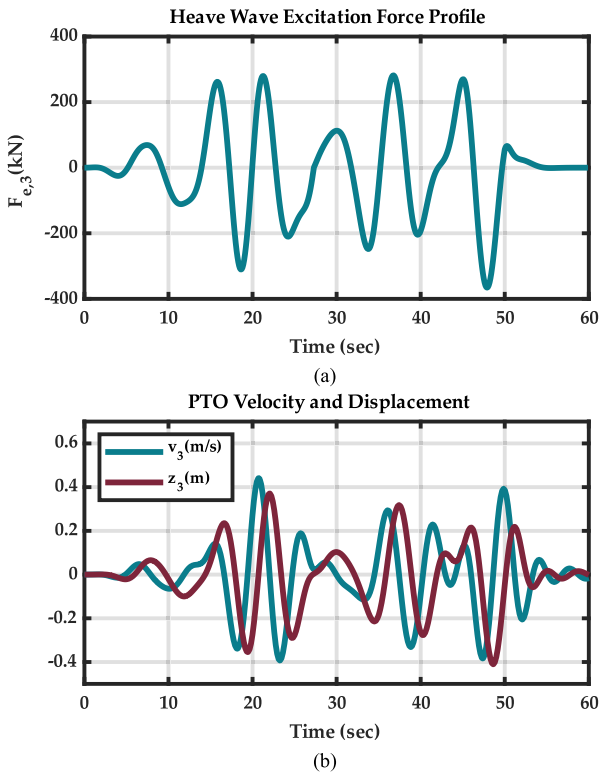

FIGURE 8. **Real-time hybrid experimental results: (a) Test profile of the wave excitation force. (b) PTO velocity and displacement.**

in Fig. 10. NMPC optimization algorithm, considering the WEC dynamics and PTO characteristics in (21), generates a PTO force that maximizes the power captured by the WEC. According to the two-tier control strategy shown in Fig. 6, if the PMSG-PTO can track the output PTO force of the NMPC,

TABLE 4. Sea States for the Experiment

Symbol	Description
Significant Wave Height [m]	0.5
Peak Period [s]	8
Wave Spectrum Type	JONSWAP (JS)
Wave Class	Irregular

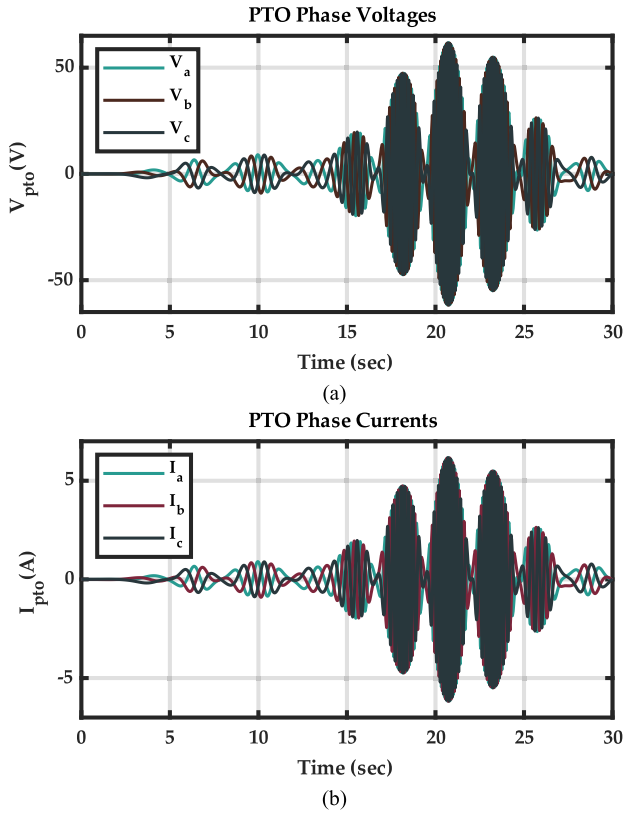

FIGURE 9. PMSG PTO generator outputs; (a) Three-phase voltage outputs from the PMSG PTO stator. (b) Three-phase current outputs from the PMSG PTO stator.

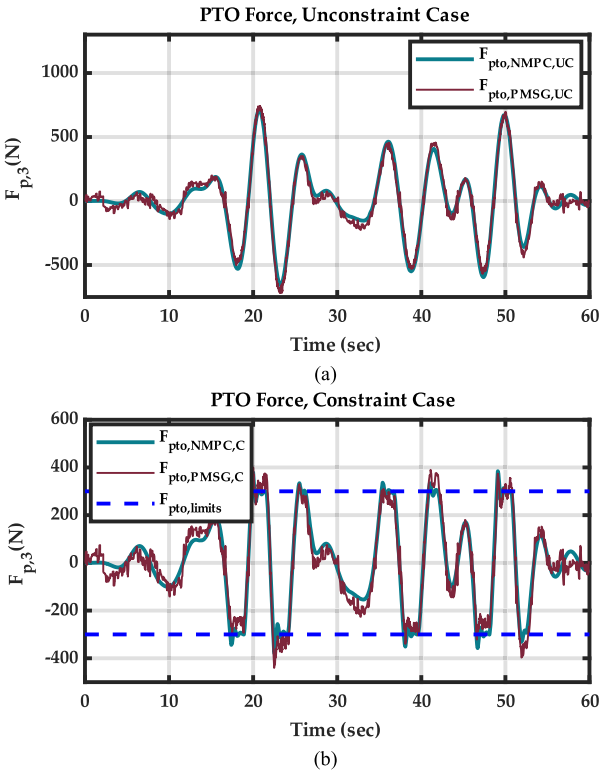

FIGURE 10. PTO Force command value by NMPC and corresponding PTO force output from the PMSG PTO; (a) Unconstrained PTO force. (b) Constrained PTO force ($|F_{pto}| \leq 300\ N$).

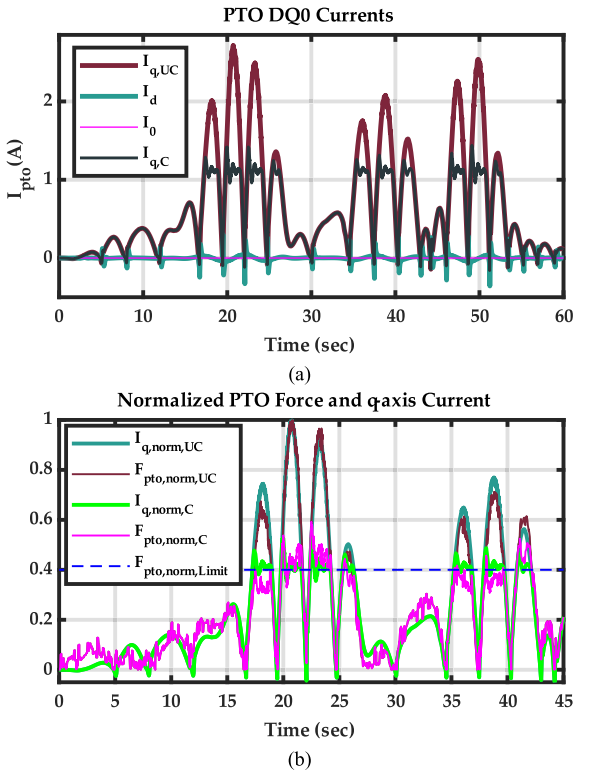

FIGURE 11. The dq0-current results with constrained and unconstrained PTO Force; (a) PTO dq0-current outputs. (b) Normalized PMSG-PTO force and q-axis current.

then power maximization is guaranteed. Two cases are considered to demonstrate the performance of the hybrid control setup; unconstrained (UC) PTO force and constrained (C) PTO force, $|F_{pto}| \leq 300\ N$, shown in Fig. 10(a) and Fig. 10(b), respectively. In either case, the output PTO force of PMSG successfully tracks the NMPC reference PTO force command.

The plots of the dq0-currents are shown in Fig. 11(a) for constraint and unconstraint PTO-force cases. Since the tracking of NMPC's PTO force command is achieved through a low-level FOC algorithm for the q-axis current regulation, Fig. 11(b) shows the normalized plots of the q-axis currents and the corresponding PTO-force output from the PMSG for constraint and unconstraint PTO-force cases, which shows the successful performance of the low-level control in terms of

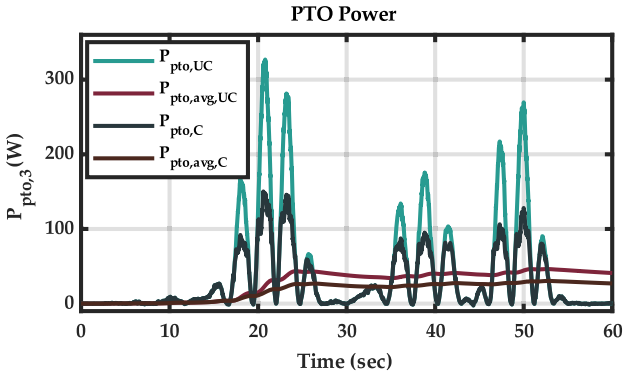

FIGURE 12. **PTO electrical power output; instantaneous and exponentially weighted moving average.**

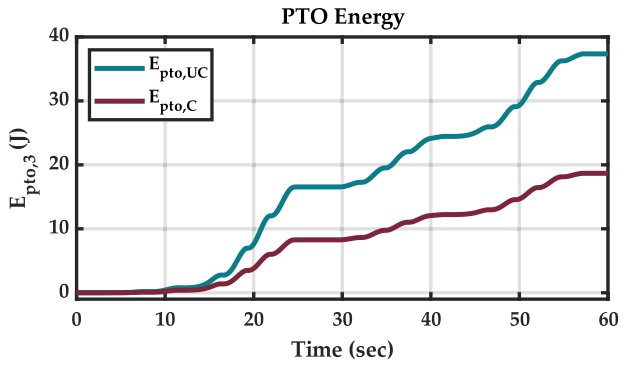

FIGURE 13. **PTO electrical energy output; (a) Unconstrained PTO force. (b) Constrained PTO force ($|F_{pto}| \leq 300\ N$).**

controlling the PTO output force using the q-axis current of PMSG.

The plots for the PTO power capture for the constraint and unconstraint PTO-force cases are shown in Fig. 12. The PTO power capture's Exponentially Weighted Moving Average (EWMA), with forgetting-factor set to 1, is plotted in Fig. 12. The plots for the PTO energy capture for the constraint and unconstraint PTO-force cases are shown in Fig. 13. These experimental results show a successful performance of the proposed hybrids set up for dry-testing ocean wave energy systems.

VI. CONCLUSION

This article presents an experimental study on developing a hybrid testing platform for wave energy systems at the Wallace Energy System and Renewables Facility (WESRF) at Oregon State University. The hybrid testing strategy was implemented by dividing the system into virtual and physical components. The physical components involved a Permanent Magnet Synchronous Generator (PMSG) PTO generator coupled to a torsional restoring spring, ocean wave emulation Linear Testbed (LTB), power electronic converter, and sensors and instrumentation. The virtual part includes a numerical model of a point absorber WEC, the NMPC control algorithm, Field Oriented Control (FOC) of the power converter, and signal processing. A single degree of freedom WEC model of a single pod from the full-scale version of the Dehlsen Associates, LLC multi-pod CENTIPOD is modeled and simulated in real-time, and NMPC is designed to maximize the electrical output power of a hardware PTO mechanism. NMPC acts as the high-level controller, and its commanded PTO force is translated into a reference q-axis current of the PMSG-PTO generator through a faster low-level FOC Loop. The full integrated testing of the hybrid scheme is performed using Speedgoat real-time performance machine interfaced with the hardware setup. The experimental results are presented, concluding with the successful performance of the proposed hybrid testing scheme. This setup can be used to experiment with advanced control algorithms for various heaving PTO mechanisms subjected to various sea states and advanced control algorithms.

REFERENCES

[1] A. Muetze and J. G. Vining, "Ocean wave energy conversion - A Survey," in *Proc. Conf. Rec. IEEE Ind. Appl. Conf. First IAS Annu. Meeting*, Oct. 2006, pp. 1410–1417, doi: 10.1109/IAS.2006.256715.

[2] J. V. Ringwood, "Wave energy control: Status and perspectives 2020," *IFAC-PapersOnLine*, vol. 53, no. 2, pp. 12271–12282, Jan. 2020, doi: 10.1016/j.ifacol.2020.12.1162.

[3] T. K. A. Brekken, A. Jouanne, and H. Y. Han, "Ocean wave energy overview and research at Oregon State University," in *Proc. IEEE Power Electron. Mach. Wind Appl.*, Jun. 2009, pp. 1–7, doi: 10.1109/PEMWA.2009.5208333.

[4] M. Leijon *et al.*, "Catch the wave to electricity," *IEEE Power Energy Mag.*, vol. 7, no. 1, pp. 50–54, Jan./Feb. 2009, doi: 10.1109/MPE.2008.930658.

[5] J. Hals, T. Bjarte-Larsson, and J. Falnes, "Optimum reactive control and control by latching of a wave-absorbing semisubmerged heaving sphere," in *Proc. 21st Int. Conf. Offshore Mechan. Arctic Eng.*, Jun. 2002, vol. 4, pp. 415–423, doi: 10.1115/OMAE2002-28172.

[6] D. Garg, W. W. Hager, and A. V. Rao, "Pseudospectral methods for solving infinite-horizon optimal control problems," *Automatica*, vol. 47, no. 4, pp. 829–837, Apr. 2011, doi: 10.1016/j.automatica.2011.01.085.

[7] R. Genest and J. V. Ringwood, "Receding horizon pseudospectral control for energy maximization with application to wave energy devices," *IEEE Trans. Control Syst. Technol.*, vol. 25, no. 1, pp. 29–38, Jan. 2017, doi: 10.1109/TCST.2016.2554524.

[8] J. V. Ringwood, G. Bacelli, and F. Fusco, "Control, forecasting and optimization for wave energy conversion," *Proc. IFAC Volumes*, vol. 47, no. 3, pp. 7678–7689, Jan. 2014, doi: 10.3182/20140824-6-ZA-1003.00517.

[9] M. Richter, M. E. Magana, O. Sawodny, and T. K. A. Brekken, "Nonlinear model predictive control of a point absorber wave energy converter," *IEEE Trans. Sustain. Energy*, vol. 4, no. 1, pp. 118–126, Jan. 2013, doi: 10.1109/TSTE.2012.2202929.

[10] N. Faedo, S. Olaya, and J. V. Ringwood, "Optimal control, MPC and MPC-like algorithms for wave energy systems: An overview," *IFAC J. Syst. Control*, vol. 1, pp. 37–56, Sep. 2017, doi: 10.1016/j.ifacsc.2017.07.001.

[11] T. K. A. Brekken, "On model predictive control for a point absorber wave energy converter," in *Proc. IEEE Trondheim PowerTech*, Jun. 2011, pp. 1–8, doi: 10.1109/PTC.2011.6019367.

[12] R. Genest and J. V. Ringwood, "A critical comparison of model-predictive and pseudospectral control for wave energy devices," *J. Ocean Eng. Mar. Energy*, vol. 2, no. 4, pp. 485–499, Nov. 2016, doi: 10.1007/s40722-016-0058-2.

[13] Y. Jia, K. Meng, L. Dong, T. Liu, C. Sun, and Z. Y. Dong, "Economic model predictive control of a point absorber wave energy converter," *IEEE Trans. Sustain. Energy*, vol. 12, no. 1, pp. 578–586, Jan. 2021, doi: 10.1109/TSTE.2020.3012755.

[14] J. B. Rawlings, D. Angeli, and C. N. Bates, "Fundamentals of economic model predictive control," in *Proc. IEEE 51st Conf. Decis. Control*, Dec. 2012, pp. 3851–3861, doi: 10.1109/CDC.2012.6425822.

[15] G. Li, "Nonlinear model predictive control of a wave energy converter based on differential flatness parameterization," *Int. J. Control*, vol. 90, no. 1, pp. 68–77, Jan. 2017, doi: 10.1080/00207179.2015.1088173.

[16] A. S. Haider, T. K. A. Brekken, and A. McCall, "Application of real-time nonlinear model predictive control for wave energy conversion," *IET Renew. Power Gener.*, vol. 15, no. 14, pp. 3331–3340, 2021, doi: 10.1049/rpg2.12257.

[17] E. Tedeschi, M. Carraro, M. Molinas, and P. Mattavelli, "Effect of control strategies and power take-off efficiency on the power capture from Sea waves," *IEEE Trans. Energy Convers.*, vol. 26, no. 4, pp. 1088–1098, Dec. 2011, doi: 10.1109/TEC.2011.2164798.

[18] G. Bacelli, R. Genest, and J. V. Ringwood, "Nonlinear control of flap-type wave energy converter with a non-ideal power take-off system," *Annu. Rev. Control*, vol. 40, pp. 116–126, Jan. 2015, doi: 10.1016/j.arcontrol.2015.09.006.

[19] A. F. O. Falcão and J. C. C. Henriques, "Effect of non-ideal power take-off efficiency on performance of single- and two-body reactively controlled wave energy converters," *J. Ocean Eng. Mar. Energy*, vol. 1, no. 3, pp. 273–286, Aug. 2015, doi: 10.1007/s40722-015-0023-5.

[20] A. S. Haider, T. K. A. Brekken, and A. McCall, "Real-time nonlinear model predictive controller for multiple degrees of freedom wave energy converters with non-ideal power take-off," *J. Mar. Sci. Eng.*, vol. 9, no. 8, Aug. 2021, Art. no. 890 doi: 10.3390/jmse9080890.

[21] "The future of testing wave energy technology," Innovation News Network, Apr. 9, 2021. Accessed: Aug. 22, 2021. [Online]. Available: https://www.innovationnewsnetwork.com/future-testing-wave-energy-technology/10570/

[22] E. E. Bachynski, V. Chabaud, and T. Sauder, "Real-time hybrid model testing of floating wind turbines: Sensitivity to limited actuation," *Energy Procedia*, vol. 80, pp. 2–12, Jan. 2015, doi: 10.1016/j.egypro.2015.11.400.

[23] "Home," VALIDHTP. Accessed: Aug. 23, 2014. [Online]. Available: https://www.validhtp.eu

[24] W. Peng *et al.*, "Hydrodynamic performance of a hybrid system combining a fixed breakwater and a wave energy converter: An experimental study," *Energies*, vol. 13, no. 21, Jan. 2020, Art. no. 5740, doi: 10.3390/en13215740.

[25] M. Steurer, F. Bogdan, W. Ren, M. Sloderbeck, and S. Woodruff, "Controller and power Hardware-In-Loop methods for accelerating renewable energy integration," in *Proc. IEEE Power Eng. Soc. Gen. Meeting*, Jun. 2007, pp. 1–4, doi: 10.1109/PES.2007.386022.

[26] R. O. Berriel, M. Shadman, Z. Wu, R. F. S. Dias, R. M. Stephan, and S. F. Estefen, "Hardware-in-the-loop development of a heaving point absorber wave energy converter using inertia emulation," *Electr. Eng.*, vol. 103, no. 6, pp. 2675–2684, Dec. 2021, doi: 10.1007/s00202-021-01244-2.

[27] J. C. C. Henriques, L. M. C. Gato, A. F. O. Falcão, E. Robles, and F.-X. Faÿ, "Latching control of a floating oscillating-water-column wave energy converter," *Renew. Energy*, vol. 90, pp. 229–241, May 2016, doi: 10.1016/j.renene.2015.12.065.

[28] L. Martinelli, P. Ruol, E. Fassina, F. Giuliani, and N. Delmonte, "A wave-2-wire experimental investigation of the new 'Seabreath' wave energy converter: The hydraulic response," *Coastal Eng. Proc.*, vol. 1, no. 34, pp. 29–39, Oct. 2014, doi: 10.9753/icce.v34.structures.29.

[29] P. Benreguig, J. Kelly, V. Pakrashi, and J. Murphy, "Wave-to-wire model development and validation for two OWC type wave energy converters," *Energies*, vol. 12, no. 20, Jan. 2019, Art. no. 3977, doi: 10.3390/en12203977.

[30] J. F. Gaspar *et al.*, "Analysis of electrical drive speed control limitations of a power take-off system for wave energy converters," *Renew. Energy*, vol. 113, pp. 335–346, Dec. 2017, doi: 10.1016/j.renene.2017.05.085.

[31] A. H. Hansen, M. F. Asmussen, and M. M. Bech, "Hardware-in-the-Loop validation of model predictive control of a discrete fluid power power Take-Off system for wave energy converters," *Energies*, vol. 12, no. 19, Jan. 2019, Art. no. 3668, doi: 10.3390/en12193668.

[32] C. Liu *et al.*, "A high-precise model for the hydraulic power take-off of a raft-type wave energy converter," *Energy*, vol. 215, Jan. 2021, Art. no. 119107, doi: 10.1016/j.energy.2020.119107.

[33] G. Bracco, E. Giorcelli, G. Mattiazzo, V. Orlando, and M. Raffero, "Hardware-In-the-Loop test rig for the ISWEC wave energy system," *Mechatronics*, vol. 25, pp. 11–17, Feb. 2015, doi: 10.1016/j.mechatronics.2014.10.007.

[34] "Hardware-in-the-loop simulation of wave energy converters based on dielectric elastomer generators | springerlink," Accessed: Jan. 9, 2022. [Online]. Available: https://link.springer.com/article/10.1007/s11012-021-01320-8

[35] C. D. Signorelli, C. Villegas, and J. V. Ringwood, "Hardware-In-The-Loop simulation of a heaving wave energy converter," *Meccanica*, 56, pp. 1223–1237, 2021.

[36] T. Potapenko *et al.*, "Power hardware in the loop real time modelling using hydrodynamic model of a wave energy converter with linear generator power take off," in *Proc. 29th Int. Ocean Polar Eng. Conf.*, Jun. 2019. Accessed: Jan. 9, 2014. [Online]. Available: https://onepetro.org/ISOPEIOPEC/proceedings/ISOPE19/All-ISOPE19/ISOPE-I-19-517/21526

[37] "Wallace energy systems & renewables facility | | oregon state university," Accessed: Aug. 23, 2021. [Online]. Available: https://wesrf.engr.oregonstate.edu/

[38] J. Prudell, M. Stoddard, E. Amon, T. K. A. Brekken, and A. von Jouanne, "A Permanent-magnet tubular linear generator for ocean wave energy conversion," *IEEE Trans. Ind. Appl.*, vol. 46, no. 6, pp. 2392–2400, Nov. 2010, doi: 10.1109/TIA.2010.2073433.

[39] B. Bosma, T. Lewis, T. Brekken, and A. Von Jouanne, "Wave tank testing and model validation of an autonomous wave energy converter," *Energies*, vol. 8, no. 8, pp. 8857–8872, Aug. 2015, doi: 10.3390/en8088857.

[40] "Vision, mission & organization," PMEC. Accessed: Jan. 11, 2022. [Online]. Available: https://www.pmec.us/mission-organization

[41] J. van Rij, Y.-H. Yu, A. McCall, and R. G. Coe, "Extreme load computational fluid dynamics analysis and verification for a multibody wave energy converter," presented at ASME 38th Int. Conf. Ocean, Offshore Arctic Eng., Nov. 2019, pp. 1–10, doi: 10.1115/OMAE2019-96397.

[42] Ecomerit Technologies, Accessed: Aug. 14, 2021. [Online]. Available: http://www.ecomerittech.com/centipod.php

[43] "WEC-Sim (Wave energy converter SIMulator) — WEC-Sim documentation," Accessed: Mar. 27, 2021. [Online]. Available: [Online]. Available: https://wec-sim.github.io/WEC-Sim/

[44] "Wamit, Inc. - The State of the art in wave interaction analysis," Accessed: Mar. 28, 2021. [Online]. Available: https://www.wamit.com/

[45] "Configure optimization solver for nonlinear MPC - MATLAB & imulink," Accessed: Jan. 12, 2022. [Online]. Available: https://www.mathworks.com/help/mpc/ug/configure-optimization-solver-for-nonlinear-mpc.html

[46] "Constrained nonlinear optimization algorithms - MATLAB & simulink," Accessed: Jan. 12, 2022. [Online]. Available: https://www.mathworks.com/help/optim/ug/constrained-nonlinear-optimization-algorithms.html

[47] C. Busca, A.-I. Stan, T. Stanciu, and D. I. Stroe, "Control of permanent magnet synchronous generator for large wind turbines," in *Proc. IEEE Int. Symp. Ind. Electron.*, Jul. 2010, pp. 3871–3876, doi: 10.1109/ISIE.2010.5637628.

[48] "Custom machines | automated laser workstations | Mundt," Accessed: Aug. 23, 2021. [Online]. Available: http://www.mundtinc.com/products/custom/

[49] "SKiiP 603 GD123-3DUL V3 | SEMIKRON," Accessed: Aug. 23, 2021. [Online]. Available: https://www.semikron.com/products/product-classes/ipm/detail/skiip-603-gd123-3dul-v3-20452028.html

ALI S. HAIDER (Member, IEEE) received the B.Sc. degree in electrical engineering from the University of Engineering and Technology, Taxila, Taxila, Pakistan, in 2008, the M.Sc. degree in electrical engineering from the Pakistan Institute of Engineering & Applied Sciences, Islamabad, Pakistan, in 2010, and the Ph.D. degree in electrical engineering from Oregon State University, Corvallis, OR, USA, in 2021, on Fulbright Fellowship. He is currently a McCain Postdoc Scholar with the University of New Brunswick, Fredericton, NB, Canada. His research interests include system modeling, control, power electronics, and electric drives with application to renewable energy systems.

TED K. A. BREKKEN received the B.S., M.S., and Ph.D. degrees from the University of Minnesota, Minneapolis, MN, USA, in 1999, 2002, and 2005, respectively. He is currently a Professor of energy systems with Oregon State University, Corvallis, OR, USA. In 1999, he studied electric vehicle motor design with Postech, Pohang, South Korea. During 2004—2005, he also studied wind turbine control with the Norwegian University of Science and Technology, Trondheim, Norway, on a Fulbright Scholarship. His research interests include control, power electronics, and electric drives, specifically digital control techniques applied to renewable energy systems. He is the Co-Director of Wallace Energy Systems and Renewables Facility. He was the recipient of the National Science Foundation CAREER Award.

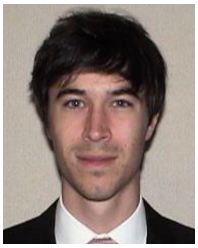

RYAN G. COE received the B.S. degree in ocean engineering and the Ph.D. degree in aerospace engineering from Virginia Tech, Blacksburg, VA, USA, in 2009 and 2013, respectively. He is currently a Senior Research Engineer with Water Power Technologies Department, Sandia National Laboratories. His research interests include hydrodynamic modeling, wave tank testing, and wave energy converter design and dynamics

GIORGIO BACELLI (Member, IEEE) received the Laurea Magistrale in electronic engineering from the Universit Politecnica delle Marche, Ancona, Italy, in 2006, and the Ph.D. degree in electronic engineering from the Center for Ocean Energy Research, Maynooth University, Maynooth, Ireland, in 2014. He is currently with Sandia National Laboratories, Albuquerque, NM, USA, working on the design and implementation of control strategies for wave energy converters.

ALAN MCCALL received the B.S. degree in mechanical engineering from the University of Toledo, Toledo, OH, USA, in 2011, and the M.Sc. degree with a focus in offshore renewable energy from the University of Strathclyde, Glasgow, U.K., in 2012. He is currently with Dehlsen Associates, LLC, Santa Barbra, CA, USA. He was leading the Centipod Wave Energy Program with Dehlsen Associates, for the past seven years. In that time, he was the Principal Investigator on several grant-funded projects in the wave energy conversion space covering a range from power take-off and controls to survivability.